Journal of the European Ceramic Society 18 (1998) 1685–1693
© 1998 Elsevier Science Limited
Printed in Great Britain. All rights reserved
PII: S0955-2219(98)00093-4
0955-2219/98/$—see front matter

Manganese-Doping of Lead Magnesium Niobium Titanate: Chemical Control of Dielectric Properties

Christopher M. Beck,[a] Noel W. Thomas[a]* and Ian Thompson[b]

[a]School of Materials, University of Leeds, Leeds, UK, LS2 9JT
[b]TAM Ceramic, PO Box 1831, Buckingham, UK, MK18 1ZP

(Received 28 April 1997; accepted 11 March 1998)

Abstract

An investigation has been carried out into the acceptor-doping of lead magnesium niobate titanate (PMNT), 0·95 $\{Pb(Mg_{1/3}Nb_{2/3})O_3\}-0{\cdot}05PbTiO_3$, through the introduction of manganese ions. These are added by co-reaction of PMNT powder with $MnCO_3$ and PbO in a single-stage reaction to sintered ceramics. The technique is found to enhance the sinterability of PMNT in less oxidising CO_2 atmospheres. Furthermore, the dielectric response of the Mn-doped ceramics depends strongly on the sintering atmosphere employed. In air, a rapid transition from relaxor to normal ferroelectric properties takes place upon addition of manganese. However, in CO_2, relaxor properties persist up to concentrations of approximately 8 mol% manganese. This difference in behaviour is attributed to varying oxidation states of the manganese ions, it being proposed that that air-sintered samples contain predominantly Mn^{3+}-ions. In CO_2-sintered samples, by comparison, the manganese ions exist in both +2 and +3 oxidation states. The relevance to the formation of dipoles, and to an understanding of relaxor ferroelectric ceramics is brought out, employing arguments based on crystal chemistry. Attention is also given to unresolved questions and to areas of future work.
© 1998 Elsevier Science Limited. All rights reserved

Zusammenfassung

Eine Untersuchung zum Akzeptor-Dotieren von Blei-Magnesium-Niobat-Titanat (PMNT), 0·95$\{Pb(Mg_{1/3}Nb_{2/3})O_3\}-0{\cdot}05PbTiO_3$, ist durch die Einführung von Mangan-Ionen durchgeführt worden. Gesinterte Keramiken werden aus Edukten PMNT, $MnCO_3$ und PbO in einer einstufigen Reaktion hergestellt. Es wird festgestellt, daß die Technik das Sintern von PMNT in reduzierenden CO_2-Atmosphären verbessert. Außerdem hängt das dielektrische Verhalten der Mn-dotierten Keramiken erheblich von der verwendeten Sinteratmosphäre ab. Während in Luft eine sofortige Umwandlung von 'relaxor' zu normalen ferroelektrischen Eigenschaften bei Zufügen von Mangan vorkommt, werden 'relaxor'-Eigenschaften bis zu Konzentrationen von 8 Mol-% Mn in CO_2 beibehalten. Dieser Unterschied kann auf die variierenden Oxidationszustände der Mangan-Ionen zurückgeführt werden, da die in Luft gesinterten Proben überwiegend Mn^{3+}-Ionen enthalten sollen. In Keramiken, die in CO_2 gesintert worden sind, sollen die Mangan-Ionen im Vergleich in sowohl +2 als auch +3 Oxidationszuständen existieren. Die Relevanz dieser Erwägungen für die Bildung von Dipolen und für das Verständnis von 'relaxor' ferroelektrischen Keramiken wird durch kristallchemische Argumente hervorgehoben. Weitere Fragen und künftige Arbeitsgebiete werden ebenfalls in Betracht gezogen.

*To whom correspondence should be addressed at WBB Technology Ltd., Watts Blake Bearne & Co plc, Park House, Courtenay Park, Newton Abbot, UK, TQ12 4PS;
e-mail: nthomas@wbb.co.uk

1 Introduction

A general technique for investigating relaxor ferroelectric ceramics is to carry out a partial substitution of the cations in a parent, model relaxor composition with foreign cations, and to monitor the effect on the dielectric properties. In this context, novel work is presented here on the synthesis and characterisation of the perovskite (ABO_3) system manganese-substituted lead magnesium niobate titanate (PMNT).

The parent composition PMNT may be represented by the formula $0{\cdot}95\{Pb(Mg_{1/3}Nb_{2/3})O_3\} - 0{\cdot}05PbTiO_3$, where the combination of lead magnesium niobate with lead titanate in the molar ratio 95:5 gives maximum relative permittivity at approximately room temperature, this being an important commercial consideration. The manganese-doped compositions to be investigated here may be represented by the formula $0{\cdot}95\{Pb(Mg_{(1-x)/3}Nb_{2(1-x)/3}Mn_x)O_{3-\delta}\} - 0{\cdot}05\ PbTi_{1-x}Mn_xO_3$, with $0 \leq x \leq 0{\cdot}1$. Here δ signifies the uncertainty in oxygen-content as a result of possible variations in the oxidation state of the manganese ion. It has the value $x(2 - \langle n_{Mn}\rangle/2)$, where $\langle n_{Mn}\rangle$ is the mean manganese oxidation number.

Since one aim of the work is to investigate a doped PMNT system which is capable of being sintered in less oxidising atmospheres, account has been taken of possible problems with electronic conduction due to loss of oxygen from the ceramic. Accordingly, it was decided to investigate *acceptor* dopants, the anticipated function of these being to reduce the concentration of free electrons in the conduction band to minimal levels. Manganese is an obvious possibility in this connection, with anticipated acceptor properties for oxidation states less than four, i.e. Mn^{2+} and Mn^{3+}. In order to highlight the importance of sintering atmosphere, two distinct sets of conditions are applied, (i) in air; and (ii) in carbon dioxide, a typical less oxidising atmosphere.

In previous work,[1] attention has been focused on B-site doping with ions in oxidation state +4, i.e. in the systems $Pb(Mg_{(1-x)/3}Nb_{2(1-x)/3}Zr_x)O_3$ and $Pb(Mg_{(1-x)/3}Nb_{2(1-x)/3}Ti_x)O_3$, with all sintering carried out in air. Here considerations of ionic radius were invoked to rationalise the observed variation in dielectric properties with dopant concentration in terms of changes in the underlying crystal structure. In particular, the values of ΔT (an empirical measure of the extent of frequency dispersion) were monitored as a function of x in both systems. A similar approach is to be adopted here in order to rationalise the observed trends in behaviour.

2 Experimental

The parent PMNT material was a 95:5 PMN-PT powder with a low sintering temperature, as supplied by TAM Ceramics, Niagara Falls, USA and designated Y5V 183U. Doped samples of composition

$$0{\cdot}95\left\{Pb(Mg_{(1-x)/3}Nb_{2_{(1-x)}/3}Mn_x)O_{3-\delta}\right\} - 0{\cdot}05\left\{PbTi_{1-x}Mn_xO_{3-\delta}\right\}$$

were prepared by combining $Mn(CO_3)_2$ and PbO powders (both BDH Analar Grade) with the PMNT powder. Compositions with values of x equal to 0, 0·0045, 0·0112, 0·0223, 0·0438, 0·065 and 0·10 were prepared, corresponding to doping levels of up to 10 mol% manganese. Samples were ball milled in isopropyl alcohol (IPA) with 3 mm zirconia (Y-TZP) media for 16 h, so that homogeneous mixing could be achieved. Particle size analysis was carried out on the slurry with a Malvern Mastersizer, in order to ensure that no significant change in particle size had occurred during milling. The slurry was subsequently dried and passed through a sieve of mesh 20 μm. Pellets were pressed at 25 MPa by means of a 19 mm pseudo-double-ended uniaxial die. No organic binders were used. Whereas the undoped PMNT used in this work could be sintered optimally to maximum density at 1000°C for 3 h, it was necessary to sinter all manganese-doped samples at 1200°C for 3 h. Two batches of sintered pellets were produced, one sintered in air and the other in CO_2. A standard muffle furnace was employed for air-sintered samples, with CO_2-sintering carried out in a tube furnace with a steady flow of CO_2 gas. Flow-rate was set with mass-flow controllers. A calibration of the furnace temperature-controller was carried out, in order to allow for the effects of the gas-flow. This was achieved by means of a thermocouple placed in the vicinity of the samples.

Microstructures of sintered pellets were examined by SEM. Quantitative analysis of grain size and porosity was carried out by means of the Imanal computerised image analysis package.[2]

Disk-shaped samples for dielectric measurement of thickness 1·5 mm were sawn out of the sintered pellets. Samples were polished using 1200 grit silicon carbide paper and cleaned with water and acetone, before being dried at 180°C for 2 h. Gold electrodes were evaporated on to both faces of the sample and subsequently covered with silver dag. Samples were allowed to dry in air before being placed in an oven at 180°C for 2 h. Measurements of complex impedance were carried out for the frequency range 100 Hz–1 MHz at temperatures between −55 and 150°C.

Powder X-ray diffraction analysis was carried out on crushed sintered pellets, using a Siemens D500 X-ray diffractometer. KCl was added to the powders as a internal standard.

3 Results

3.1 Powder X-ray diffraction

Diffraction patterns for all fourteen sintered samples (seven sintered in air and seven in CO_2) indi-

cated that, to a good approximation, a cubic unit cell with lattice parameter a_o could be adopted in all cases. Plots of a_o versus x are given in Fig. 1. It is seen that this parameter remains approximately constant for air-sintered samples. By comparison, a_o increases with concentration of manganese dopant for samples sintered in CO_2.

3.2 Sintered density

Densities of sintered pellets, expressed as a fraction of the maximum density, are plotted against manganese concentration in Fig. 2 Here, maximum densities have been calculated from the observed lattice parameters (Fig. 1), assuming a δ-value equal to x. This is tantamount to making the approximation that all manganese ions are in the +2 oxidation state. Doping with manganese appears to aid densification in CO_2 at [Mn]-levels of up to 6·5 mol%. However there is a rapid decrease in sintered density between 6·5 and 10 mol% [Mn], falling from 95 to 87% of maximum density. Air-sintered samples have lower densities than their counterparts sintered in CO_2, with the exception of the 10 mol% doped sample. Again sintered density falls between the 6·5 and 10 mol% doped samples. Image analysis of SEM-micrographs revealed differences in both grain-size and porosity between the $x = 0{\cdot}0112$ and $x = 0{\cdot}10$ compositions sintered in CO_2, corresponding to the maximum and minimum observed densities. Sintered grain diameter was found to vary typically between 3 and 8 μm, falling off in the 10 mol% doped sample to 2–3 μm.

3.3 Dielectric measurements

The variation of relative permittivity, ε_r with temperature is given in Fig. 3(a) and (b) for a representative composition ($x = 0{\cdot}0223$) sintered in air and CO_2, respectively. The air-sintered sample exhibits smaller permittivity levels than its CO_2-sintered counterpart. The latter shows, moreover, a characteristic relaxor response, with shifts in the permittivity peak to higher temperatures with increasing frequency.

Differences in dielectric response between air- and CO_2-sintered samples are observed for all manganese concentrations. It is seen in Fig. 4 that the temperature of maximum permittivity, $T(\varepsilon_{r,max})$, rises sharply in air-sintered samples at the lowest manganese substitution-level, $x = 0{\cdot}0045$, remaining approximately constant at all higher manganese-concentrations. By comparison, the rise in $T(\varepsilon_{r,max})$ with [Mn] is gradual in CO_2-sintered samples, with a cross-over between the CO_2- and air-sintered curves at a manganese doping-level of approximately 7%. Figure 5 shows that relative permittivity levels at 1 kHz increase initially in CO_2-sintered samples, followed by a decrease with rising [Mn]-concentration with x)0·0112. The corresponding $\varepsilon_{r,max}$-values are considerably lower in air-sintered samples, showing an overall decrease with increasing manganese concentration. The two curves tend towards convergence as [Mn] reaches 10 mol%. Further insight into the differences between CO_2- and air-sintered samples is provided by Fig. 6, in which the parameter ΔT is used as a simple indicator of

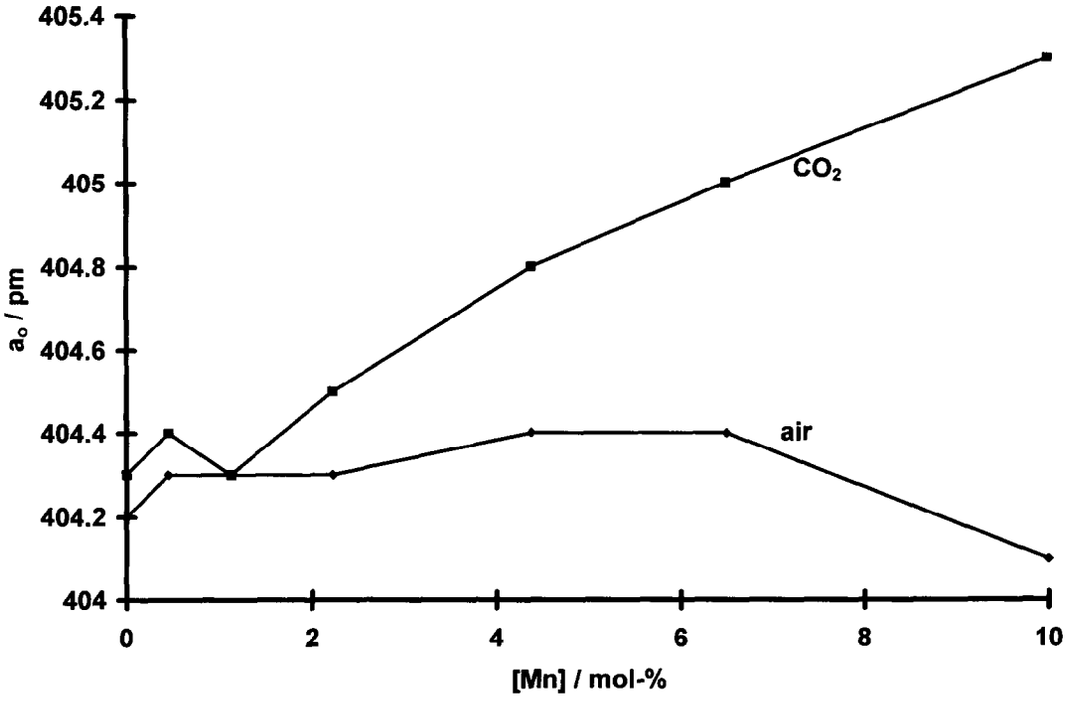

Fig. 1. Variation of cubic lattice parameter a_o with manganese concentration for samples sintered at 1200°C in air and in carbon dioxide.

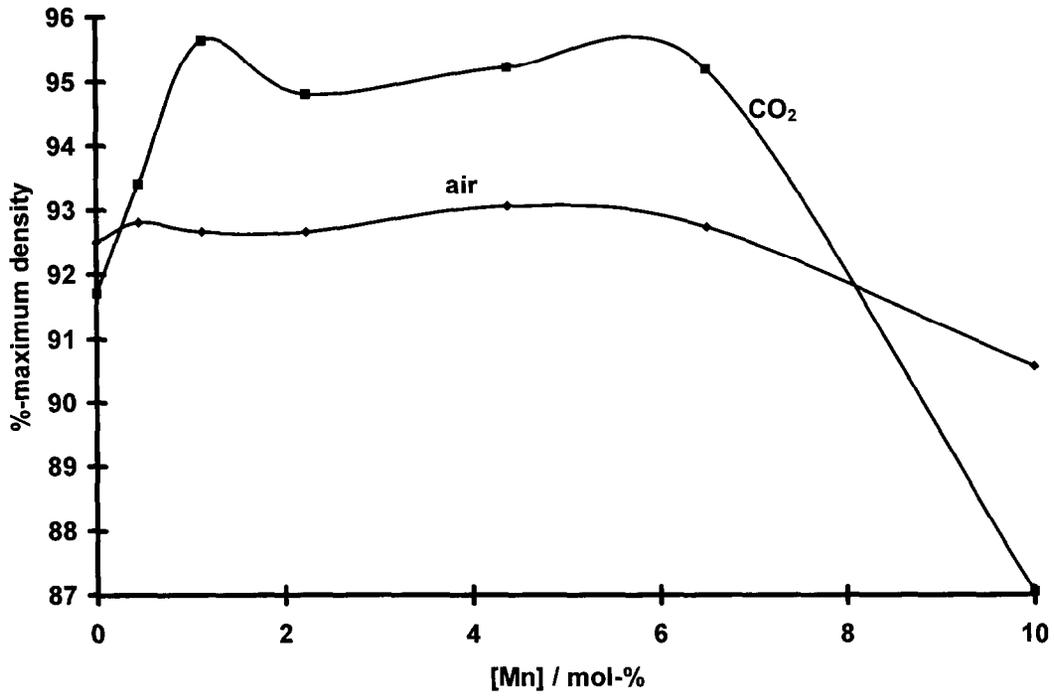

Fig. 2. Variation of density of pellets (sintered at 1200°C) expressed as a percentage of calculated maximum density, with manganese concentration.

the degree of frequency-dispersion, i.e. relaxor behaviour:

$$\Delta T = T(\varepsilon_{r,\max})_{1\ \mathrm{MHz}} - T(\varepsilon_{r,\max})_{100\ \mathrm{Hz}} \qquad (1)$$

In air-sintered samples, this parameter falls immediately to negligible values in Mn-doped samples, in contrast to the behaviour observed in CO_2-sintered samples, where a significant degree of relaxor behaviour is maintained at doping levels of up to 5 mol% [Mn]. At the highest doping-level of 10 mol%, a convergence is observed of the curves for air- and CO_2-sintered ceramics at a small *negative* value.

4 Discussion

The above results, concerning lattice parameters, densification and dielectric properties, show great sensitivity to whether samples are sintered in air or in CO_2. In summary, relaxor properties are maintained in the less oxidising CO_2 environment, whereas the oxidising conditions of air promote a rapid transition to normal ferroelectric properties. A rationalisation of these observations is now proposed, in which the ability of the manganese ion to be stabilised in several oxidation states is taken into account.

The manganese doping has been carried out with $MnCO_3$ (manganese oxidation state +2) as the starting reactant, for which the properties on heating in several controlled atmospheres have been previously investigated.[3] For a furnace heating rate of 12°C per min, dissociation of the carbonate was found to occur in air at approximately 650°C, followed by oxidation of the resulting MnO at ca. 825°C. From X-ray diffraction, the oxidised product was identified as Mn_2O_3, corresponding to a manganese oxidation state of +3. Although X-ray diffraction suggested the subsequent decomposition in air of Mn_2O_3 to Mn_3O_4 at 1000°C, evidence of this decomposition could only be obtained in DTA for samples subjected to preheating in air for 24 h at 650°C. No such evidence was obtained for straightforward heating rates of up to 12°C per min. When heated in carbon dioxide, $MnCO_3$ decomposed to MnO at 650°C, as in air, but no oxidation was found to occur to Mn_2O_3 at higher temperatures. The final product at 1000°C in CO_2 was identified by XRD as Mn_3O_4 (i.e. Mn_2O_3.MnO) with a small amount of MnO.

The significance of these observations for this study is as follows. In air, the oxidation state of the manganese ion can be expected to increase from +2 to +3, prior to reaction to form the desired perovskite product. It remains an open question as to whether dissociation of Mn_2O_3 to $MnO.Mn_2O_3$ occurs as an intermediate reaction at ca. 1000°C, or whether reaction to form the perovskite phase proceeds directly, with manganese still in the +3 state. (Some subsequent formation of Mn^{2+} within the perovskite phase is also conceivable.) In carbon dioxide, by comparison, the extent of the oxidation to the +3 state will be much smaller. Here no direct oxidation to Mn_2O_3 is expected, so that any

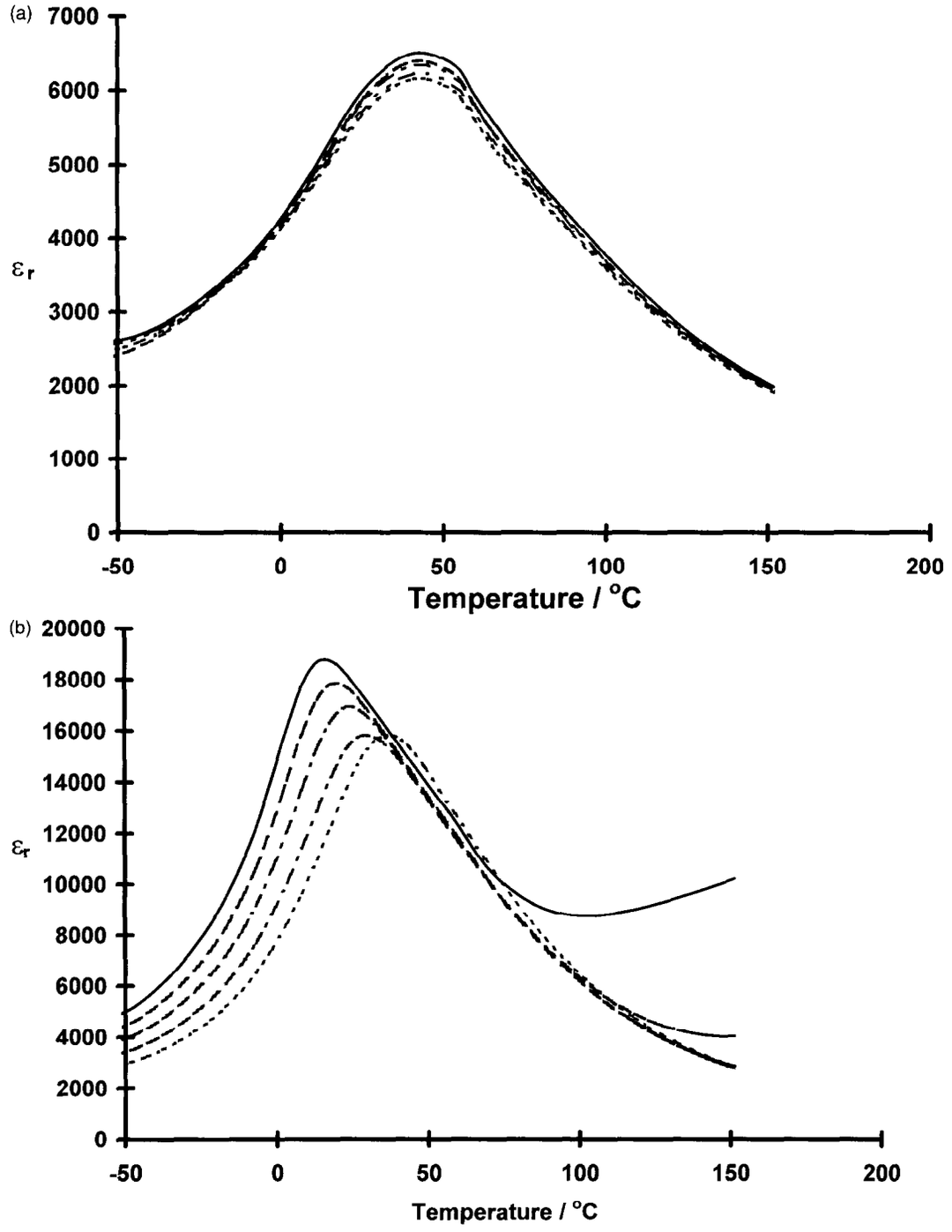

Fig. 3. (a) Variation of relative permittivity with temperature for the $x = 0{\cdot}0223$ composition sintered in air. The continuous curve corresponds to a signal field of frequency 100 Hz, with dashed lines representing frequencies 1 kHz, 10 kHz, 100 kHz and 1 MHz. The length of the dashes decreases with increasing frequency. (b) Variation of relative permittivity with temperature for the $x = 0{\cdot}0223$ composition sintered in CO_2. Frequency is indicated as in Fig. 3(a).

Mn^{3+} ions in the final product would either be by direct oxidation within the perovskite phase, or alternatively via $MnO.Mn_2O_3$ as an intermediate. In summary, the concentration of Mn^{3+} ions is expected to be much greater in the air-sintered than in the CO_2-sintered systems.

This postulated dependence of manganese oxidation state on sintering conditions provides the key to rationalising the observed differences in properties between samples sintered in air and in CO_2. The ionic radii of Mn^{2+} and Mn^{3+} are 67 and 58 pm, respectively, for six-fold coordination in the (expected) low spin-state,[4] these ions substituting for $0{\cdot}95(Mg_{1/3}Nb_{2/3})$, $0{\cdot}05Ti$. Thus the mean ionic radius of the B-site ions prior to substitution is $0{\cdot}95/3r^{VI}(Mg) + 0{\cdot}95 \times 2/3r^{VI}(Nb) + 0{\cdot}05r^{VI}(Ti)$. Taking values 72, 64·5 and 60·5 pm for the Mg^{2+}, Nb^{5+} and Ti^{4+} ions, respectively, the mean radius is calculated to be 66·675 pm. Thus, in terms of ionic radii alone, Mn^{2+} ions would be expected to have a slightly expansionary effect on the crystal structure, with Mn^{3+} ions a rather more dramatic

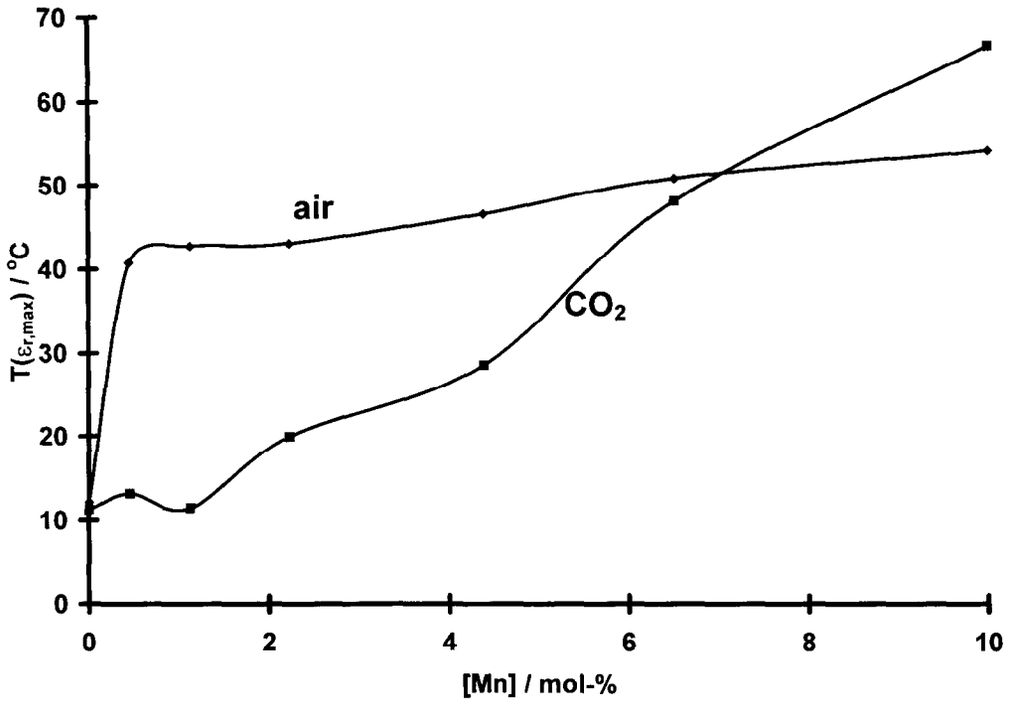

Fig. 4. Variation of temperature of maximum permittivity, $T(\varepsilon_{r,max})$, with manganese concentration for samples sintered in air and in carbon dioxide.

effect in reducing the size of the unit cell. Assuming that, in CO_2-sintered ceramics, all manganese ions are in the +2 oxidation state, the B-ion radius is predicted to increase from 66·675 to 66·675 $\times 0{\cdot}9 + 67 \times 0{\cdot}1 = 66{\cdot}7075$ pm between the undoped and 10 mol% doped samples, an increase of a mere 0·05%. This is to be compared with the increase in a_o shown in Fig. 1 from 404·3 to 405·3 pm, some 0·25%. This relatively small discrepancy can be attributed to inaccuracies in the assumed ionic radii and/or non-random substitution of Mn^{2+} ions over B-sites, with investigation of these factors outside the scope of this article.

Of more significance, however, is the absence of a marked decrease in a_o with increasing manganese substitution in air-sintered samples: $a_o = 404{\cdot}2$ for $x = 0$ and 404·1 pm for $x = 0{\cdot}01$, with intermediate values of *up to* 404·4 pm. Thus the overall decrease

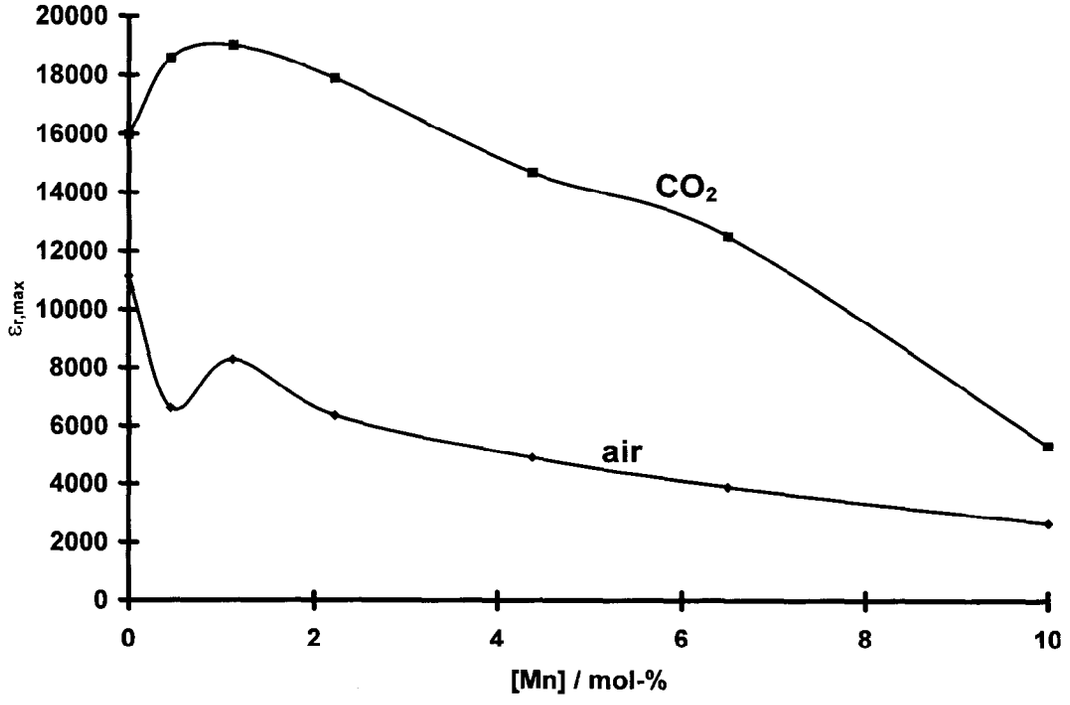

Fig. 5. Variation of maximum relative permittivity at 1 kHz, $\varepsilon_{r,max}$, with manganese concentration for samples sintered in air and in carbon dioxide.

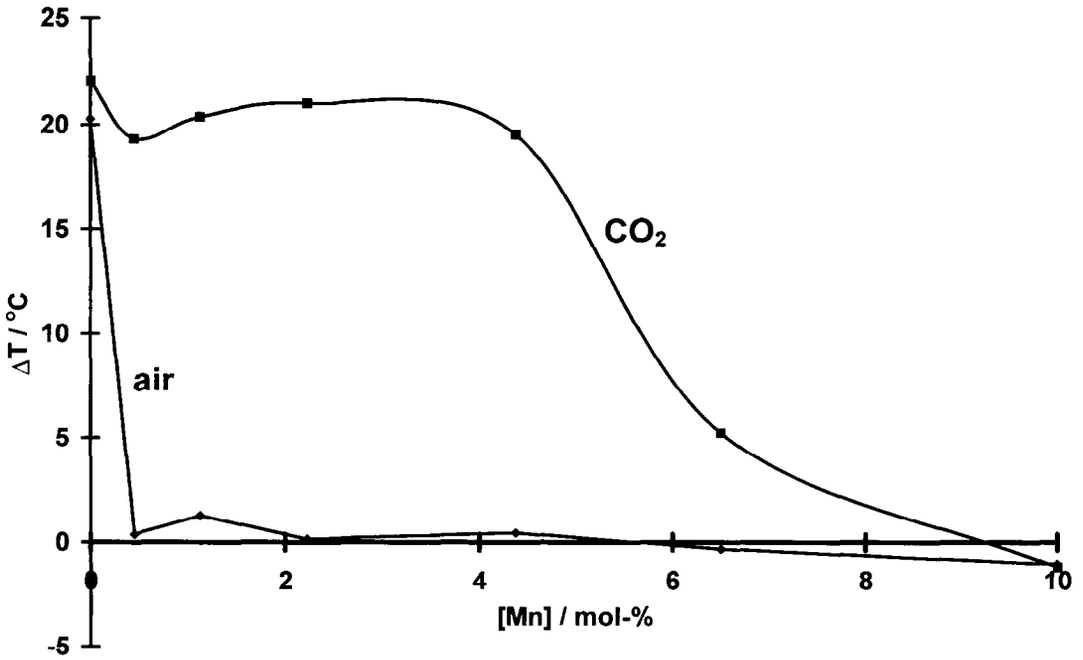

Fig. 6. Variation of frequency dispersion parameter, ΔT, with manganese concentration for samples sintered in air and in carbon dioxide.

in a_o is only 0·025%, whereas the mean B-ion radius, assuming all manganese ions to be in the +3 state, is predicted to be reduced from 66·675 pm to $66{\cdot}675\times0{\cdot}9 + 58\times0{\cdot}1 = 65{\cdot}8075$ pm. This corresponds to a reduction of 1·32%. Since this substitution has a smaller effect than would be expected from straightforward considerations of ionic radii, the inference is that the Mn^{3+} ions will be located inside octahedra which are too large for them to be located at the O_6-octahedral centres. Rather, Mn^{3+} ions will have considerable off-centre displacements, which will be associated with large local electric dipole moments.

These suppositions concerning the different effects of Mn^{2+} and Mn^{3+} substitution are consistent with the crystal chemistry and properties of other ferroelectric perovskite systems. Owing to the filling of space by AO_{12} cuboctahedra and BO_6 octahedra in ABO_3 systems, the volumes of these two octahedra, V_A and V_B are unable to vary independently of each other. Furthermore, for systems with untilted octahedra, as is the case here, $V_A/V_B = 5$. Thus, in the case of smaller cations entering B-sites, the volumes of their BO_6 octahedra are essentially determined by that of the AO_{12} cuboctahedra, i.e. $V_B = V_A/5$.[5,6] In the present system, the volume of the BO_6-octahedra will thus be largely controlled by the coordination requirements of the A-site lead ions, which do not change with increasing Mn^{3+} concentration. By comparison, the Mn^{2+} ion increases the volume of its BO_6 octahedron, V_B, also increasing V_A in proportion. In general, for structures with untilted octahedra, the unit cell volume is given by $6V_B$.[5]

The postulated $Mn(III)O_6$-dipoles are thought to be responsible for the considerable differences in the dielectric properties of air- and CO_2-sintered samples shown in Figs 3–6. The presence of Mn^{3+} ions gives rise to the rapid and immediate fall in ΔT observed in air-sintered samples in Fig. 6. This is also seen clearly in Fig. 3, where the relaxor-properties of the CO_2-sintered $x = 0{\cdot}0223$ sample are to be compared with the absence of relaxation in the corresponding air-sintered sample. Also worthy of comment is the increase in ε_r-values in Fig. 3(b), for frequencies 100 Hz and 1 kHz, at the high-temperature side of the peak. Since this is most evident at the lower frequency, it is likely to be attributable to a thermally activated conduction process.

There are likely to be two possible mechanisms for this conduction. The first corresponds to an electron-hopping process, for which the presence of both Mn^{2+} and Mn^{3+} ions would be necessary. If this is the underlying cause of this behaviour, the presence of both Mn^{2+} and Mn^{3+} ions in the CO_2-sintered sample is implied. By comparison, the absence of an increase in ε_r-values at 100 Hz and 1 kHz in the air-sintered samples suggests a complete oxidation of the manganese ions to the +3 state. Alternatively, the conduction could be due to oxygen ion conduction, which should be greater in the CO_2-sintered sample because of the expected higher concentration of oxygen vacancies compared to corresponding air-sintered material.

Complementary to the rapid fall in ΔT in manganese-substituted samples sintered in air is the rapid rise in $T(\varepsilon_{r,max})$ observed in Fig. 4. This can

be attributed to the immediate existence of sufficient numbers of $Mn(III)O_6$-dipoles. These are thought to perform a 'bridging function' between the polarisation clusters responsible for the relaxor-type response in unsubstituted PMNT. As has been argued previously,[17] these polarisation clusters may be visualised as regions of interconnected NbO_6 (and TiO_6) octahedra, with $Nb^{5+}(Ti^{4+})$ ions displaced off-centre within distorted octahedra. In the case of PMNT,[1] the function of the Ti^{4+} ions and associated TiO_6 dipoles is to increase the size of these polarisation clusters, thereby reducing ΔT from 23·70 to 7·80°C between PMN and 80 mol%(PMN)—20 mol% (PT). Clearly the $Mn(III)O_6$-dipoles are much larger than their TiO_6 counterparts, reducing ΔT from 20·28 to 0·39°C at a substitution level of just 0·45 mol% manganese in 95 mol%(PMN)–5 mol%(PT). Since the degree of relaxation is negligible, it may be argued that the polarisation vectors of the polarisation clusters (as in undoped PMNT) are oriented by the $Mn(III)O_6$-dipoles in such a way that the whole material can respond coherently to an electric field. Thus macroscopic ferroelectric domains have been formed. The effectiveness with which the $Mn(III)O_6$-dipoles perform this function signifies their magnitude and concomitant long-range interactions.

Further support for the co-existence of Mn^{2+} and Mn^{3+} ions in CO_2-sintered samples is provided by the gradual rise in $T(\varepsilon_{r,max})$ observed in Fig. 4. The CO_2-based curve ultimately crosses that of the air-sintered samples at a manganese concentration of approximately 7 mol%. Similarly, in Fig. 6, ΔT falls gradually in CO_2-sintered samples, approaching that of air-sintered ceramics at higher manganese-levels. A critical Mn^{3+} concentration for the formation of macroscopic ferroelectric domains is therefore proposed, which, because of the lower proportion of Mn^{3+} to Mn^{2+} ions in CO_2-sintered systems, is only reached at higher manganese substitution-levels.

Two issues remain: (i) the cross-over in $T(\varepsilon_{r,max})$-curves for CO_2- and air-sintered samples at a manganese concentration of approximately 7 mol%; and (ii) the generally higher values of $\varepsilon_{r,max}$ observed in CO_2-sintered samples. Clearly the first of these cannot be rationalised in terms of higher $[Mn^{3+}]$ concentrations in the CO_2-sintered samples, so an alternative mechanism is required. An obvious compositionally-based mechanism would rest on the expected greater concentration of oxygen vacancies in these samples, since more of the manganese ions will be in the +2 state than in the air-sintered counterparts. As a consequence of the three dimensional BO_6 octahedral network, the presence of oxygen vacancies will not lead to a reduction in unit cell volume, but rather to the presence of additional space within the crystal structure. The B-ions would thus be able to show larger off-centre displacements, with associated increased dipole moments and higher values of $T(\varepsilon_{r,max})$. The presence of oxygen vacancies, in itself, will alter the distribution of negative charges within the crystal structure, also affecting the dipole moments. The local environments of the B-ions in the presence of oxygen vacancies remain to be investigated, by techniques such as EXAFS, EELS and MASNMR. It is anticipated that one oxygen vacancy is introduced per Mn^{2+} ion, with two Mn^{3+} ions required to give rise to an oxygen vacancy. It is unknown whether these vacancies are located adjacent to manganese ions, or whether they are to be found preferentially in the vicinity of magnesium, niobium or titanium ions.

The generally higher values of $\varepsilon_{r,max}$ in CO_2-sintered samples are clearly connected with their polarisation cluster type of structure, in comparison to the macroscopic ferroelectric domain structure proposed for air-sintered samples. The observation of larger $\varepsilon_{r,max}$-values is frequently correlated with relaxor properties, although there is, as yet, no straightforward theoretical framework for the interpretation of this phenemenon.

More work remains to be carried out on this system. It is not known whether oxidation from the Mn^{2+} to the Mn^{3+} state takes place within a manganese oxide phase, or whether this occurs within the perovskite phase which forms at higher temperatures. The stage at which this oxidation takes place is likely to be dependent on reaction conditions. The question is relevant, however, to the control of second phase formation. From considerations of ionic radii, it is expected that Mn^{2+} ions are more likely to go into solid solution in the perovskite phase than Mn^{3+} ions. Thus this initial work points towards the oxidation of manganese *in situ* within the perovskite phase.

There is also scope for determining the minimum Mn^{3+} concentration required to give rise to a sharp, ferroelectric response. This would require an examination of the dielectric properties of air-sintered samples at low dopant-levels.

It is also of interest to determine whether the postulated ferroelectric domains in the air-sintered samples really exist. Direct evidence for these could be sought by chemical etching, followed by SEM. Indirect evidence for these would be found by an investigation of the hysteresis behaviour of the samples. The poling of the air-sintered samples also remains to be investigated, with a view to their being piezoelectric materials of high activity. The ageing characteristics of poled samples, and comparison with other known materials, would also

provide indirect information on the domain structure of the air-sintered Mn-doped PMNT system.

Mn-doping levels beyond 10 mol% are still to be investigated. Finally, the effect of other first-row transition metal ions apart from manganese on PMN or PMNT systems remains to be examined. The magnetic susceptibility of these materials is also of interest, since the manganese ions have magnetic dipole moments which vary with oxidation state. The question remains as to whether the magnetic dipoles are independent of one another, or whether ordering, exchange interactions will come into play at higher manganese concentrations and/or lower temperatures. Work on all these questions is currently in progress.

5 Conclusion

It has been shown that doping PMNT with manganese is an effective technique for increasing its sinterability in less oxidising atmospheres, such as CO_2. This is of relevance to the continued development of dielectric ceramics which can be co-sintered with base metal electrodes. The introduction of manganese into PMNT, however, has profound effects on its dielectric properties. These have been interpreted in terms of the presence of Mn^{3+} and Mn^{2+} ions, together with oxygen vacancies. Mn^{3+} ions are considered to be responsible for a transition between relaxor and normal ferroelectric properties. It is proposed that, through the formation of large dipoles, these ions are able to effect a change from a polarisation cluster type of structure to one consisting essentially of macroscopic ferroelectric domains. This manganese-doping technique, with its ability to switch between relaxor and normal ferroelectric properties, offers great potential for the chemical control of dielectric properties, along with the possible generation of novel, highly active piezoelectric ceramics.

Acknowledgements

Financial support from Cookson Group plc. for one of us (C.M.B) is gratefully acknowledged. Thanks are due to the Analytical Department of the former Cookson Technology Centre, and also to Mr C. Hood and Dr M. Rand for technical assistance and valuable discussions. The work of Professor R. Stevens (University of Bath) and Drs J. Bultitude and M. Chu (TAM Ceramics Inc.) in initiating work in this area is also acknowledged.

References

1. Tavernor, A. W. and Thomas, N. W., The dependence on chemical composition of the relaxor response of zirconium-substituted lead magnesium niobate ceramics. *J. Europ. Ceram. Soc.*, 1994, **13**, 121–127.
2. Thomas N. W., Advances in image analysis techniques for ceramics. *Brit. Ceram. Proc.*, 1997, **57**, 1–5.
3. Dressel, W. M. and Kenworthy, H., Thermal behaviour of manganese minerals in controlled atmospheres. US Department of the Interior, Bureau of Mines, Report 5671, 1996, p. 21.
4. Shannon, R. D., Revised effective ionic radii and systematic studies of interatomic distances in halides and chalcogenides. *Acta Crystallogr.*, 1976, **A32**, 751–767.
5. Thomas, N. W., Crystal structure-physical property relationships in perovskites. *Acta Crystallogr.*, 1989, **B45**, 337–344.
6. Thomas, N. W., The Influence of crystal chemistry on the ferroelectric and piezoelectric properties of perovskite ceramics.. *Brit. Ceram. Proc.*, 1994, **52**, 1–12.
7. Thomas, N. W., Beyond the tolerance factor: harnessing X-ray and neutron diffraction data for the compositional design of perovskite ceramics. *Brit. Ceram. Trans*, 1997, **96**, 7–15.